



HAL
open science

Optimization of a Planar All-Polymer Transistor for Characterization of Barrier Tissue

Marc Ramuz, Kaleigh Margita, Adel Hama, Pierre Leleux, Jonathan Rivnay,
Ingrid Bazin, Roisin M. Owens

► **To cite this version:**

Marc Ramuz, Kaleigh Margita, Adel Hama, Pierre Leleux, Jonathan Rivnay, et al.. Optimization of a Planar All-Polymer Transistor for Characterization of Barrier Tissue. *ChemPhysChem*, 2015, 16 (6, SI), pp.1210-1216. 10.1002/cphc.201402878 . hal-02914248

HAL Id: hal-02914248

<https://hal.science/hal-02914248>

Submitted on 4 Dec 2023

HAL is a multi-disciplinary open access archive for the deposit and dissemination of scientific research documents, whether they are published or not. The documents may come from teaching and research institutions in France or abroad, or from public or private research centers.

L'archive ouverte pluridisciplinaire **HAL**, est destinée au dépôt et à la diffusion de documents scientifiques de niveau recherche, publiés ou non, émanant des établissements d'enseignement et de recherche français ou étrangers, des laboratoires publics ou privés.

Optimization of a Planar All-Polymer Transistor for Characterization of Barrier Tissue

Marc Ramuz,^{*[a]} Kaleigh Margita,^[b] Adel Hama,^[a] Pierre Leleux,^[c] Jonathan Rivnay,^[a] Ingrid Bazin,^[d] and Róisín M. Owens^[a]

The organic electrochemical transistor (OECT) is a unique device that shows great promise for sensing in biomedical applications such as monitoring of the integrity of epithelial tissue. It is a label-free sensor that is amenable to low-cost production by roll-to-roll or other printing technologies. Herein, the optimization of a planar OECT for the characterization of barrier tissue is presented. Evaluation of surface coating, gate biocompatibility and performance, and optimization of the geometry of the transistor are highlighted. The conducting poly-

mer poly(3,4-ethylenedioxythiophene):poly(styrene sulfonate), which is used as the active material in the transistor, has the added advantage of allowing significant light transmission compared to traditional electrode materials and thus permits high-quality optical microscopy. The combination of optical and electronic monitoring of cells shown herein provides the opportunity to couple two very complementary techniques to yield a low-cost method for in vitro cell sensing.

Keywords: barrier tissue · conducting polymers · electrochemistry · organic electrochemical transistors · sensors

1. Introduction

The organic electrochemical transistor (OECT), first described by White et al.,^[1] has recently seen a renaissance for biomedical applications. In contrast to the classical organic field-effect transistor, in the OECT the electrolyte is an integral part of the device structure.^[2] The active material is based on poly(3,4-ethylenedioxythiophene):poly(styrene sulfonate) (PEDOT:PSS), which has the ability to conduct both electronic and ionic carriers, and thus offers a unique platform for sensing in biomedical applications. A key feature of the OECT is its ability to act as an ion-to-electron converter that can be operated at low voltages. The device operates on the principle that the electronic drain current in the PEDOT:PSS channel is modulated by the ionic current between the electrolyte and the conducting polymer. A second key feature of the use of conducting-polymer devices is the ease with which they can be fabricated, especially because it has been demonstrated that optimization

of the device geometry can greatly enhance sensing capabilities.^[3-5]

In electrically inactive cells, electronic measurements can be used as a measure of cell coverage and differentiation, and thus as a measure of cell viability. Additionally, electronic measurements can interrogate the integrity of epithelial (and some endothelial) cell layers, which serve as functional barriers in the body by tightly controlling the flux of ions. Ion transport between cells is regulated by protein structures known as tight junctions. The ability to measure the function of tight junctions provides information about barrier tissue and is indicative of certain disease states. Hence, the effect of drugs/toxins on these barrier tissues can be assessed by measuring the electrical resistance of the cell layers (transepithelial resistance), which correlates well with cell viability and is an earlier determinant than cytotoxicity assays such as the lactate dehydrogenase assay.^[6-8] Until recently, the majority of methods for electrically monitoring cell health in vitro have been used in basic research. However, there is increasing demand for reliable techniques for high-throughput screening, with a preference for label-free methods.^[9,10] Further, the development of accurate in vitro models that can replace animal tests requires a competent validation method. Electronic methods are particularly promising because they are dynamic and can yield time-resolved data for both acute and chronic exposure. This can have applications in medical diagnostics, food and water safety, homeland security, and environmental protection. The advantage of electrical monitoring is that it is amenable to dynamic measurement, as opposed to the static and time-consuming biochemical or immunofluorescence methods.

One of the electrical methods currently used to characterize barrier tissue is electrical impedance spectroscopy (EIS), which has long been used to determine mechanisms of reactions oc-

[a] Dr. M. Ramuz, A. Hama, Dr. J. Rivnay, Dr. R. M. Owens
Department of Bioelectronics
Ecole Nationale Supérieure des Mines CMP-EMSE
880 route de Mimet, 13541 Gardanne (France)
E-mail: ramuz@emse.fr

[b] K. Margita
Department of Chemistry, Newberry College
Newberry, SC 29108 (USA)

[c] Dr. P. Leleux
Microvitae Technologies, Pôle d'Activité Y. Morandat
13120 Gardanne (France)

[d] Dr. I. Bazin
Ecole des mines d'Alès, LGEl, 6 avenue de Clavière
30319 Alès Cedex (France)

curing at electrode/electrolyte interfaces.^[11] EIS can be employed to measure the capacitance and resistance of cell layers in a more automated and reproducible fashion. This technology has made significant contributions in the field but requires relatively expensive equipment and still has limitations in terms of temporal resolution and sensitivity. EIS does not allow high-resolution imaging due to the typical use of gold electrodes. Transistors provide an alternative to the use of simple electrodes for monitoring cells both *in vivo*^[12] and *in vitro*.^[13] A key difference in the use of a transistor as the sensing element, as opposed to a conventional electrode, is the inherent amplification associated with the former, whereby small changes in the ionic flux are integrated and amplified in the drain current. We previously demonstrated the use of a PEDOT:PSS-based OECT for monitoring the integrity of barrier tissue to provide a novel method for assessing toxicology of compounds *in vitro*.^[13,14] A human colon cancer cell line was used as a model of the gastrointestinal epithelium. Cells were grown on permeable hanging Transwell filters until fully differentiated and then integrated with the OECT by means of a top gate electrode. The cell monolayers act as a partial barrier to the ionic current. This current is in turn transduced by the OECT, and thus the channel current is a measure of the barrier function of the cells. However, the use of a top-gate device causes certain inconveniences in fabrication and operation. The use of organic materials has the potential for development of cheap and possibly disposable devices, because these materials are compatible with large-scale roll-to-roll processing. However, to fully take advantage of these low-cost production methods, it is necessary to produce a planar device rather than a top-gate device. Another motivation for moving away from a top-gate device is the toxic nature of conventional Ag/AgCl electrodes observed on incubation of cells with these electrodes for long-term measurements.^[14] A further disadvantage of a device in which the cells are grown on a filter is the difficulty in obtaining high-resolution optical images. The use of a planar device to monitor cell arrays has been investigated by Yan and co-workers, but these devices do not measure baseline barrier-tissue function.^[15,16]

This work focuses on the development of a long-term dynamic measurement of barrier tissue and presents a series of optimizations required in terms of gate choice, geometrical features, and improvement of cell adhesion. Herein, we present evidence for the advantages of using PEDOT:PSS both for gate and channel, and thus fabricating a fully planar device, and further show enhanced biocompatibility of the resulting device. Optimization of the adhesion of cells seeded directly on the OECT is highlighted, since it is a key parameter for acquiring valuable data about the barrier tissue. Contrary to cells grown on filters, our system is compatible with established optical characterization techniques that are common in cell biology. It is thus possible to simultaneously measure the barrier resistance corresponding to its integrity and record optical in-

formation on the cell morphology. The biosensor presented herein provides a vehicle for fundamental research in life sciences, facilitates studies on barrier tissue and the factors affecting its integrity, and allows for the development of realistic *in vitro* cell models for drug discovery and toxicology.

2. Results and Discussion

The biosensor consists of a glass substrate with patterned gold/PEDOT:PSS as channel (Figure 1). The gate electrode can

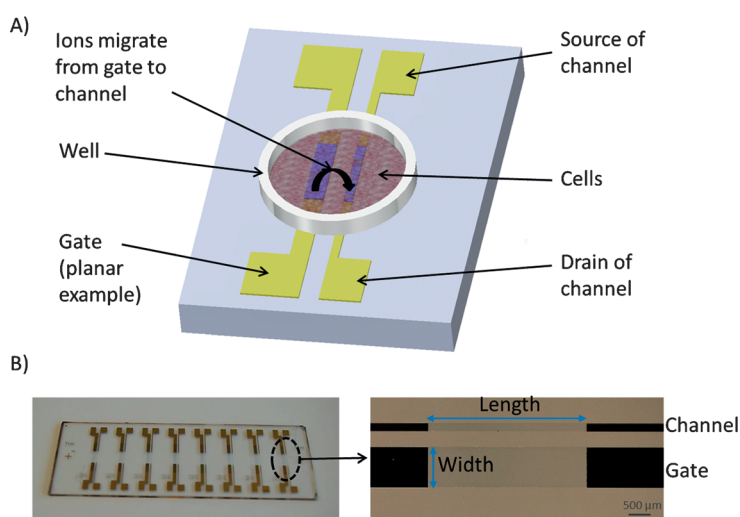


Figure 1. A) Schematic of the OECT with a planar PEDOT:PSS gate. Active materials were based on PEDOT:PSS, and gold was used as contacts. Cells grew directly on the PEDOT:PSS inside a polydimethylsiloxane well. B) Left: Image of the planar OECTs. Eight OECTs were fabricated on a $75 \times 25 \text{ mm}^2$ glass substrate. Right: gate and channel active areas were made entirely of PEDOT:PSS (arrows) and were in the same plane.

be placed on top of the electrolyte, as is usually reported,^[13,14,17] or in the same plane as the channel, as shown in Figure 1A. A thin (100 nm) layer of gold is used to improve the contact measurement, but the active area is based on PEDOT:PSS alone. MDCK-I cells were chosen for this experiment as a robust and well-characterized cell line that is known to differentiate and create a functional barrier to ions on planar substrates.^[18] The cells were seeded into a well affixed to the OECT. On application of a square pulse voltage of $V_{GS} = 0.3 \text{ V}$ between the gate (G) and source (S) electrodes, cations from the electrolyte (cell medium) are forced into the channel and dedope it.^[17,19] The barrier tissue formed by the MDCK-I cells partially blocks the ion flow and thus slows down the dedoping process. By measuring the channel-current response to the gate pulse, it is therefore possible to detect the ability of the cell layer to block ion flow into the device, and by corollary to assess the quality of the cell layer.

Two key parameters of the OECT for barrier-tissue characterization are detailed in this work: the dedoping modulation of the source-drain current and the time constant τ . The current modulation of dedoping is an intrinsic parameter of a defined OECT, the maximization of which allows increases in the dynamic range and the sensitivity of the biosensor. The τ value is

obtained by fitting the channel current response to a gate square pulse. This parameter is used to quantify the quality of the barrier tissue. It is similar to the time constant used in the charge/discharge of a resistor–capacitor circuit in electronic systems. A large τ value represents a longer time taken to dedope the channel and is thus associated with a healthy, functional barrier-tissue layer. In contrast, a small τ value is expected in the absence of cells or in the presence of cells that have little or no barrier function.

2.1. Gate Choice

As mentioned above, the characterization of barrier tissue by using the OECT was previously performed with an Ag/AgCl gate electrode immersed in the cell medium as a top gate.^[2,8,13,13,14] However, Ag/AgCl was found to deteriorate the barrier properties of an epithelial cell layer and so could not be used for long-term experiments (> 12 h).^[14] To assess the biocompatibility of different materials for use as gate electrode, a variety of gate electrodes were tested by immersing them in the cell medium (nonplanar configuration). Gate electrodes consisting of PEDOT:PSS, Ag, Ti, Cr, Au, Ni, Ag/AgCl, and

Cu were evaluated for biocompatibility. To assess biocompatibility, MDCK-I cells were seeded into tissue-culture-treated plastic wells and allowed to grow for 3 days. Into each of these wells, a gate electrode of 9 mm² was placed in contact with the medium at day zero, while avoiding contact with the cells. No bias was applied, and the toxicity of the gates to cell growth was monitored by optical imaging.

Figure 2A shows light-microscopy images of the cells taken 3 days after seeding. Using the cell morphology and coverage as a crude indicator of the biocompatibility of the different electrodes reveals that PEDOT:PSS, Ag, Ti, Cr, and Au do not appear to have a detrimental effect on the formation of the MDCK-I cell layer. However, in the case of Ni, Ag/AgCl, and Cu, the cells failed to proliferate and indeed appeared to die when cultured in the presence of these materials. Although the use of Ag/AgCl electrodes is widespread in electrophysiology, it is important to highlight the cytotoxic effects of this material on cells, at least for long-term experiments, which has previously been documented.^[20,21]

An important function of the gate electrode is the ability to properly dedope the PEDOT:PSS channel. The different electrodes were used as gates on a deliberately large PEDOT:PSS

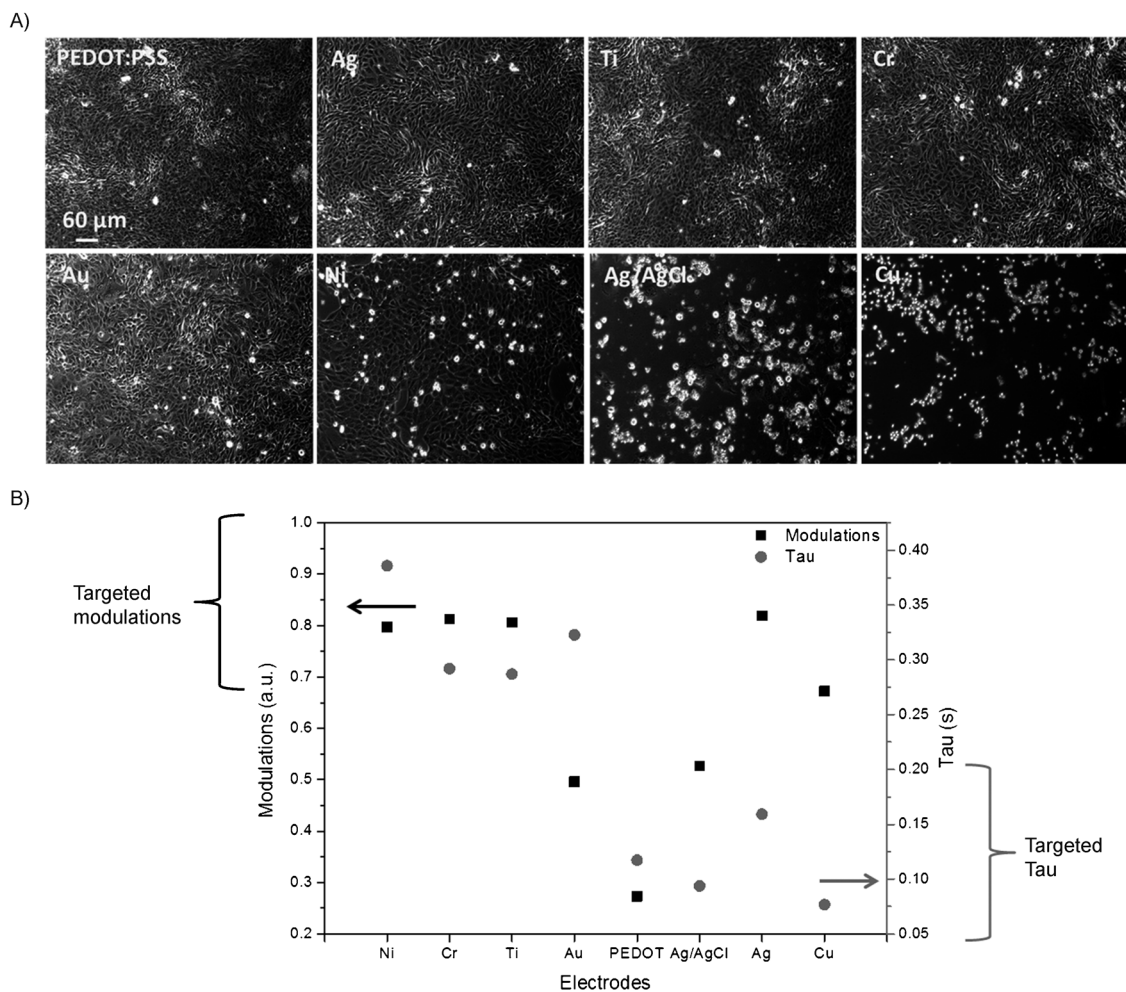


Figure 2. Biocompatibility and electrical performance of the various gate electrode materials immersed in the electrolyte (nonplanar configuration). Original data are provided in Figure S1. A) Images of MDCK-I cells grown in culture plates in the presence of different gate materials (at day 3). B) Modulations in current and τ parameter for each gate electrode material without cells. The area of the channel was 10 mm², and the area of the gate was 9 mm² in all cases.

channel (10 mm²) in order to detect how fast (τ value) these electrodes can operate and how much current modulation they generate when used as gate for our application. In this experiment, the intrinsic characteristics of the OEET were observed in the absence of cells. Thus, a high current modulation and a low τ value were targeted, which correspond to a large dynamic range and fast dedoping of the channel, respectively. As shown in Figure 2B, Ni, Cr, Ti, and Au have high τ values. However, they cannot be used as gate electrodes, since they cannot dedope the channel fast enough, which would result in a device of lower sensitivity and decreased dynamic range. The four other electrodes tested (PEDOT:PSS, Ag/AgCl, Ag, and Cu) show low τ values that make them usable as gate electrodes.

Owing to their combinations of electrical-performance data (Figure 2B) and biocompatibility (Figure 2A), Ag/AgCl and Cu must be discarded as gate choices, leaving PEDOT:PSS and Ag as suitable gate electrodes for the planar OEET barrier-tissue sensor. Although Ag shows superior current modulation, PEDOT:PSS has the major advantage that it can be processed during the same fabrication step as the channel. Moreover, by increasing the gate/channel area ratio, it is possible to dramatically increase the current modulation when PEDOT:PSS is used as the gate.

2.2. Geometry Optimization

Previous work by Malliaras and co-workers on the geometry of the OEET demonstrated that maintenance of a low gate/channel area ratio allows the potential drop to occur mainly at the gate/electrolyte interface, and the dedoping of the channel is thus limited.^[22]

This is explained by the unbalanced potential distribution between the gate and the channel. Another explanation for the small modulation at gate/channel ratios of less than eight is that the PEDOT:PSS gate electrode becomes fully oxidized and limits the extent of reduction of PEDOT:PSS in the transistor channel.^[23,24] In agreement with these works, we observed that, by increasing the aspect ratio of the gate with respect to the channel by up to a factor of eight, the current modulation was improved. Figure 3A shows the current modulation achieved (in the absence of cells) while increasing the gate width with respect to the channel width, but keeping the length of both gate and channel identical. In this data set the channel width was 200 μm and the channel length 4 mm. At ratios greater than eight, a plateau is reached corresponding to complete dedoping of the channel. However, at large gate/channel ratios, the drop of potential occurs at the channel interface, and this demonstrates the proficiency of PEDOT:PSS as a gate.

To assess the effect of geometry on the τ value, τ measurements were carried out with MDCK-I cells 4 days after seeding. Without cells (Figure 2B, PEDOT:PSS gate), τ was about 0.1 s,

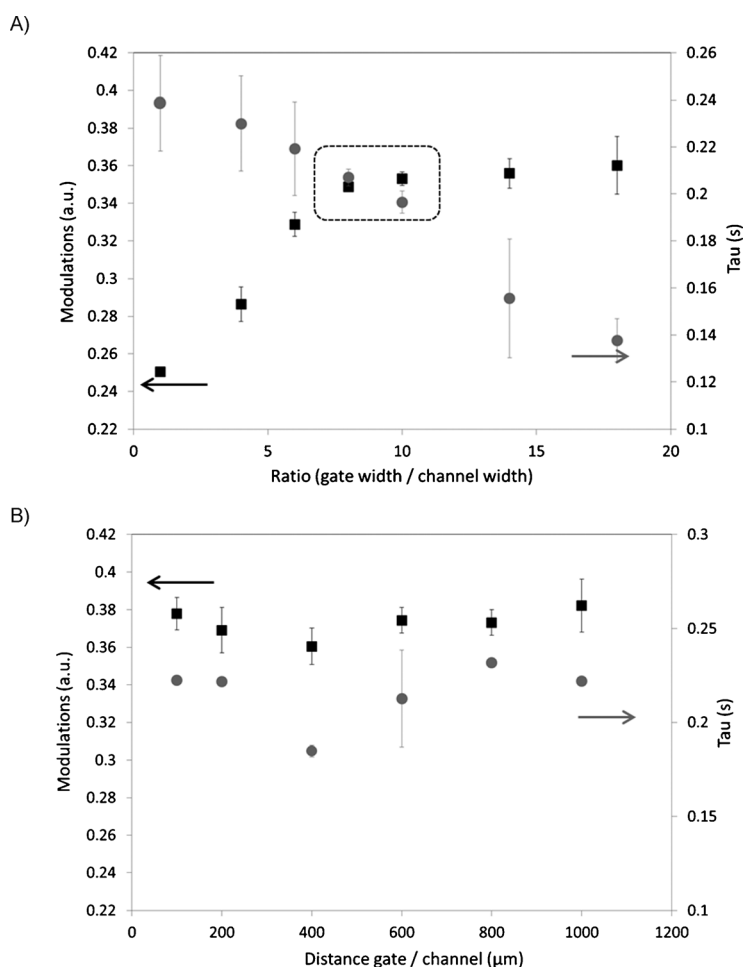


Figure 3. Variation of geometrical parameters of the planar OEET with a PEDOT:PSS gate. A), B) Current modulation data measured on OEETs in the absence of cells; τ values were measured on OEETs with MDCK-I cells 4 days after seeding. A) Evolution of current modulation and τ for various ratios (gate width/channel width). Channel and gate length were constant at 4 mm. B) Influence of the gate/channel distance.

which means the channel of the OEET was dedoped rapidly. The cells act as a barrier that increases the time τ to dedope the channel. With cells, the dedoping time τ must be as high as possible so that the cases cells/no cells can be properly distinguished. In this way, the biosensor has a large dynamic range of measurement. As shown in Figure 3A, τ decreases continuously with increasing gate/channel ratio. In this geometrical configuration, current modulation and by corollary the ion flux between gate and channel is reduced. Thus, the OEET becomes more sensitive to small changes, such as the presence of cells, which tend to improve its sensitivity and dynamic range. A tradeoff between high current modulation and high τ value in the presence of cells is thus found for gate/channel ratios of 8–10, as indicated by the boxed area in Figure 3A.

Another important aspect of the geometry of the planar OEET for barrier-tissue characterization is the distance between the gate and the channel. As shown in Figure 3B, in the absence of cells the current modulation remains constant with increasing distance between the channel and the gate up to

a maximum of 1 mm. This demonstrates that the movement of cations from the gate to the channel is not a limiting factor for proper operation of the OECT. This geometrical parameter was also studied in the presence of cells. The τ value was measured 4 days after seeding of MDCK-I cells on the devices. Figure 3B shows the absence of variation in τ when the distance between gate and channel varies from 100 μm to 1 mm. As expected, the cations do not move laterally between adjacent cells. In that case the τ parameter would have increased with increasing distance between gate and channel. Without cells, τ was less than or equal to 0.1 s (Figure S2 in the Supporting Information). This provides evidence that the passage of the ions occurs predominantly through the cell layer. More precisely, the cations flow from the gate through the cells to the medium, and then again through the cell layer from the medium to the channel. This dual passage of ions through the cell layer improves the sensitivity.

2.3. Cell Adhesion

Another important aspect of device optimization is the adhesion of the cells to the active layer of the OECT. Increased interaction with or adhesion of the cells to the surface can reduce the cell-interface resistance and thus improve the measurement quality.^[18,25] Coating of substrates with different extracellular matrix (ECM) proteins is a commonly used technique to improve adhesion to the surface. We coated the device surfaces with a number of different ECM-derived proteins, namely, collagen I, gelatin, poly-lysine, and fibronectin.

Figure 4A shows that, in the absence of cells, the τ value of the OECT is identical for each coating and is about 25 ms, that means the ECM-derived proteins do not influence the behavior of the transistor and do not generate any resistance. This is expected due to the highly porous nature of these protein layers. However, in the presence of cells (Figure 4B), the τ value is modified according to the protein used, with the exception of collagen I. Gelatin and poly-lysine slightly improve adhesion, with a 20% increase of the τ value. In the case of fibronectin, the τ value is greatly enhanced, by a factor of almost three compared with PEDOT:PSS alone. This increase in τ value may be attributable to a reduction of the space between the basal membrane of the cell and the PEDOT:PSS film,^[26,27] which increases the overall cell-layer resistance.

2.4. Combined Optical and Electrical Measurements

The planar OECT described herein allows simultaneous recording of the electrical behavior of a barrier tissue and optical imaging. In Figure 5, we demonstrate the use of the optimized device for monitoring the disruption of a functional barrier-tissue layer by addition of trypsin. Trypsin is an enzyme that is well-known to indiscriminately cleave all protein types and therefore is used to detach cells from surfaces. In Figure 5A, trypsin was added at $t=0$ min. After 6 min, the normalized τ values start to decrease constantly until $t=45$ min, at which the barrier function of the MDCK-I cell layer is completely compromised. The decrease in τ represents a disruption of the bar-

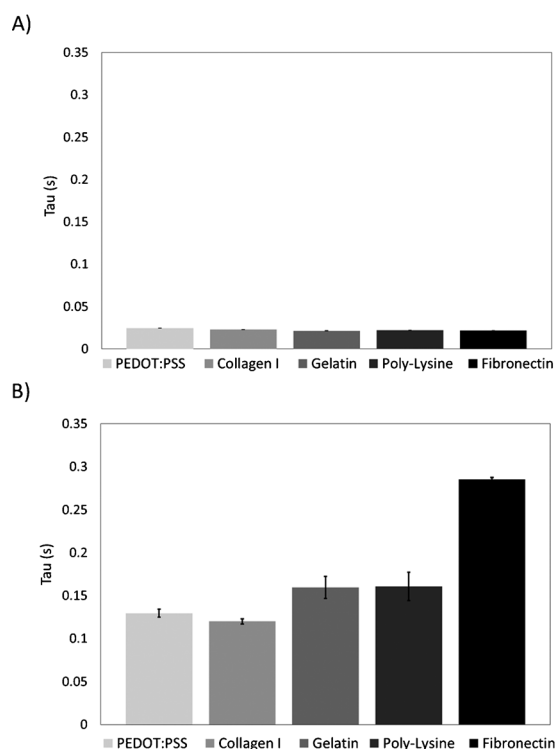


Figure 4. Optimization of cell adhesion on a planar PEDOT:PSS gate device. A) Effect of different adhesion-promoter proteins on the τ value in the absence of cells. B) Effect of different adhesion-promoter proteins on the τ value in the presence of MDCK-I cells measured at day 4. All OECTs used were identical (channel and gate length of 4 mm; gate width/channel area ratio of 8). Original data are provided in Figure S3.

rier properties of the cell layer resulting from faster dedoping of the channel on application of a square gate-voltage pulse. In the corresponding optical images, cell detachment is first observed at $t=30$ min, that is, 24 min after τ begins to decrease. As expected, the electrical recording provides greater resolution in monitoring the barrier-tissue properties.

3. Conclusions

OECTs show great promise as a tool to characterize barrier-tissue properties of cells. The planar OECT reported herein has two great advantages: the first is the facile fabrication process, and the second is the ability to record optical images simultaneously with electrical characterization of the barrier tissue. We validated the use of a planar OECT with PEDOT:PSS as both channel and gate for barrier-tissue sensing. The use of PEDOT:PSS facilitates the fabrication process and has the potential to lower device cost. For proper working operation, the voltage drop at the PEDOT:PSS can be compensated by increasing the gate/channel ratio to improve the current modulation. We further demonstrated that operation of the planar OECT is greatly improved by coating with fibronectin, undoubtedly due to increased adhesion of the cell layer on the PEDOT:PSS film. Finally, we demonstrated the operation of the optimized device for monitoring the disruption of functional MDCK-I barrier tissue grown on the planar OECT, with in-

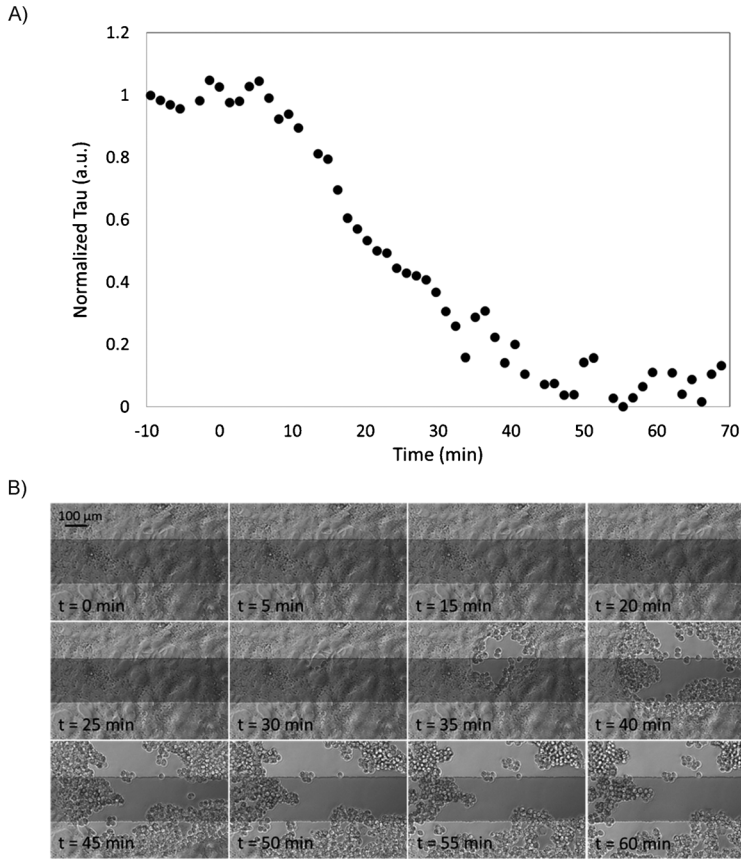


Figure 5. Simultaneous recording of the electrical and optical barrier behavior after addition of trypsin. MDCK-I cells were previously grown on an optimized OECT for 4 days. Then, the OECT with cells was placed under a microscope in time-lapse mode while the electrical signal was simultaneously recorded. A) The normalized τ parameter measured after addition of trypsin. Trypsin 0.1X was added at $t=0$ min. Original data are provided in Figure S4. B) Corresponding optical images. The darker band in the middle of the images is the channel of the OECT. The complete video is shown in Figure S4.

creased temporal resolution compared to the simultaneously collected optical images. Future work will focus on exploiting the combined optical and electronic approach by labeling the tight junctions and toxic agents in order to directly correlate biological phenomena of barrier disruption at the molecular level with measured electrical signals.

Experimental Section

OECT Fabrication

The conducting polymer formulation consisted of PEDOT:PSS (Heraeus, Clevios PH 1000), supplemented with ethylene glycol (Sigma Aldrich, 0.25 mL for 1 mL of PEDOT:PSS solution), 4-dodecylbenzenesulfonic acid ($0.5 \mu\text{L mL}^{-1}$), and 3-glycidoxypropyltrimethoxysilane (10 mg mL^{-1}). On a clean glass substrate ($75 \times 25 \text{ mm}$), gold source and drain contacts were patterned by lift-off lithography and then thermally evaporated. Photoresist S1813 (MicroChem Corp.) was spin-coated at 3000 rpm for 30 s on the glass substrate. Patterns were defined by photolithography (chrome mask and Mask Aligner). MF-26A was used as developer. Then, 5 nm and 100 nm of chromium and gold, respectively, were evaporated. Finally, the photoresist was lifted off in an acetone bath under sonication for 1 h, which left the substrate with the source and drain Au contacts only. PEDOT:PSS channels were patterned by a Parylene

peel-off technique described previously^[28] to give a PEDOT:PSS channel thickness of 460 nm. Following PEDOT:PSS deposition, devices were baked for 1 h at 140°C under atmospheric conditions. A PDMS well of 0.5 cm^2 (hole diameter of 0.8 cm) defined the cell-growth area.

Electronics

All measurements were done by using the PEDOT:PSS film as the channel and cell medium (see below) as the electrolyte. Experiments were performed in ambient atmosphere when no cells were involved. In the presence of cells, measurements were done inside a biological incubator with temperature and CO_2 level of 37°C and 5%, respectively. Measurement parameters were chosen to avoid exposing the cell layers to a voltage drop greater than 0.5 V, because high voltages have been shown to damage bilayer membranes.^[29] The measurements on the OECTs were performed with a Keithley 2612 Source Meter and customized Labview software. OECT data were collected using the following parameters: $V_{\text{DS}} = -0.2 \text{ V}$, with a 2 s pulse of $V_{\text{GS}} = 0.3 \text{ V}$ and a 30 s duty cycle.

Data Analysis

The modulation was calculated as the channel current I_{DS} with applied gate voltage minus I_{DS} without applied gate voltage, divided by I_{DS} without applied gate voltage [Eq. (1)]:

$$\text{Modulation} = \frac{I_{(V_g > 0)} - I_{(V_g = 0)}}{I_{(V_g = 0)}} \quad (1)$$

Data were analyzed by using a customized Matlab program to isolate and fit the time constant for each pulse. The time constant τ was extracted by performing a least-squares fit of the data from each pulse current response to Equation (1) [Eq. (2)]:

$$I_d = \left\{ \alpha_1 \left[1 - e^{-\frac{(t-t_0)}{\tau}} \right] + \alpha_2 \left[1 - e^{-\frac{(t-t')}{\tau'}} \right] \right\} \quad (2)$$

where α is a constant scaling term describing the magnitude of the current response, t_0 the time at which the pulse starts, and τ is the time constant discussed above. Equation (1) was found to fit the experimental data well, both with and without cells, as already demonstrated previously.^[14] The second exponential term, described by a time offset t' and time constant τ' , is incorporated to describe the long-time evolution of the drain current, likely associated with the OECT rather than the barrier tissue. The contribution

from the second, slow exponential does not vary significantly over the timescale of the experiment.

The data were then normalized by using the following equation: $NR = (\tau_{no\ cells} - \tau) / (\tau_{no\ cells} - \tau_{cells})$, where τ_{cells} is the RC rise time of the drain current in response to the application of the gate voltage of a barrier-forming monolayer and $\tau_{no\ cells}$ refers to τ value in response to the application of the gate voltage of no barrier, with the dataset subsequently normalized to a to [0,1] scale, where 1 corresponds to intact cell layer and 0 to a disrupted one.

Cell Culture

MDCK-I cells from HPA culture collection (catalogue no. 86010202) were seeded at a density of 5×10^4 cells per well. Cells were routinely maintained at 37 °C in a humidified atmosphere of 5% CO₂ in Dulbecco's modified Eagle's medium low glucose (Advanced DMEM Reduced Serum Medium 1X, Invitrogen) with 2 mM glutamine (Glutamax-1, Invitrogen), 10% fetal bovine serum (Invitrogen), 0.5% PenStrep (PenStrep 100X, Invitrogen), and 0.1% gentamicin (Gentamicin 100X, Invitrogen).

Coating

ECM proteins such as collagen I, gelatin, poly-lysine, and fibronectin were prepared at a concentration of 150 $\mu\text{g mL}^{-1}$ in phosphate-buffered saline (PBS). The solution was coated on the wells of the OECT and left for 90 min inside a cell culture incubator at 37 °C. Then, wells were emptied and rinsed twice with PBS.

Trypsin Experiments

MDCK-I cells were grown directly on top of the OECT. They were maintained inside the incubator for 4 days for full confluence and stable barrier properties. Then, a substrate with the OECTs seeded with cells was placed onto an Axio Observer Z1 microscope from Carl Zeiss MicroImaging equipped with humidified incubator XL multi SI from PeCon GmbH. After 1 h of stabilization, recording of the electrical signal of the OECT and time-lapse optical recording were started. After about 15 min and while continuing the recording, the desired concentration of trypsin (Trypsin 0.1X) was added to the well; this corresponds to time $t=0$ min in Figure 5. Note that Trypsin 1X corresponds to 0.05 % trypsin with 0.02% ethylenediaminetetraacetic acid.

- [1] H. S. White, G. P. Kittlesen, M. S. Wrighton, *J. Am. Chem. Soc.* **1984**, *106*, 5375–5377.
- [2] J. Rivnay, R. M. Owens, G. G. Malliaras, *Chem. Mater.* **2014**, *26*, 679–685.
- [3] F. Cicoira, M. Sessolo, O. Yaghmazadeh, J. A. DeFranco, S. Y. Yang, G. G. Malliaras, *Adv. Mater.* **2010**, *22*, 1012.
- [4] P. C. Hutter, T. Rothlander, A. Haase, G. Trimmel, B. Stadlober, *Appl. Phys. Lett.* **2013**, *103*, 043308.
- [5] D. Khodagholy, J. Rivnay, M. Sessolo, M. Gurfinkel, P. Leleux, L. H. Jimison, E. Stavrinidou, T. Herve, S. Sanaur, R. M. Owens, G. G. Malliaras, *Nat. Commun.* **2013**, *4*, 1–6.
- [6] J. A. Guttman, B. B. Finlay, *Biochim. Biophys. Acta BBA - Biomembr.* **2009**, *1788*, 832–841.
- [7] J. McLaughlin, P. J. Padfield, J. P. H. Burt, C. A. O'Neill, *Am. J. Physiol. Cell Physiol.* **2004**, *287*, C1412–1417.
- [8] S. A. Tria, L. H. Jimison, A. Hama, M. Bongo, R. M. Owens, *Biochim. Biophys. Acta BBA - Gen. Subj.* **2013**, *1830*, 4381–4390.
- [9] M. F. Peters, K. S. Knappenberger, D. Wilkins, L. A. Sygowski, L. A. Lazor, J. Liu, C. W. Scott, *J. Biomol. Screening* **2007**, *12*, 312–319.
- [10] C. W. Scott, M. F. Peters, *Drug Discovery Today* **2010**, *15*, 704–716.
- [11] I. Giaever, C. R. Keese, *Proc. Natl. Acad. Sci. USA* **1984**, *81*, 3761–3764.
- [12] D. Khodagholy, T. Doublet, P. Quilichini, M. Gurfinkel, P. Leleux, A. Ghestem, E. Ismailova, T. Hervé, S. Sanaur, C. Bernard, G. G. Malliaras, *Nat. Commun.* **2013**, *4*, 1575.
- [13] L. H. Jimison, S. A. Tria, D. Khodagholy, M. Gurfinkel, E. Lanzarini, A. Hama, G. G. Malliaras, R. M. Owens, *Adv. Mater.* **2012**, *24*, 5919–5923.
- [14] S. A. Tria, M. Ramuz, M. Huerta, P. Leleux, J. Rivnay, L. H. Jimison, A. Hama, G. G. Malliaras, R. M. Owens, *Adv. Healthcare Mater.* **2014**, *3*, 1053–1060.
- [15] P. Lin, F. Yan, J. J. Yu, H. L. W. Chan, M. Yang, *Adv. Mater.* **2010**, *22*, 3655.
- [16] C. Yao, C. Xie, P. Lin, F. Yan, P. Huang, I.-M. Hsing, *Adv. Mater.* **2013**, *25*, 6575–6580.
- [17] D. A. Bernards, G. G. Malliaras, *Adv. Funct. Mater.* **2007**, *17*, 3538–3544.
- [18] C. M. Lo, C. R. Keese, I. Giaever, *Biophys. J.* **1995**, *69*, 2800–2807.
- [19] P. Lin, F. Yan, H. L. W. Chan, *ACS Appl. Mater. Interfaces* **2010**, *2*, 1637–1641.
- [20] C. Greulich, S. Kittler, M. Epple, G. Muhr, M. Köller, *Langenbecks Arch. Chir.* **2009**, *394*, 495–502.
- [21] S. Kittler, C. Greulich, J. Diendorf, M. Koller, M. Epple, *Chem. Mater.* **2010**, *22*, 4548–4554.
- [22] O. Yaghmazadeh, F. Cicoira, D. A. Bernards, S. Y. Yang, Y. Bonnassieux, G. G. Malliaras, *J. Polym. Sci. Part B* **2011**, *49*, 34–39.
- [23] P. Andersson, R. Forchheimer, P. Tehrani, M. Berggren, *Adv. Funct. Mater.* **2007**, *17*, 3074–3082.
- [24] O. Larsson, *Empirical Parameterization of Organic Electrochemical Transistors*, Institutionen för Teknik och Naturvetenskap, Linköpings Universitet, **2004**.
- [25] D. Braun, P. Fromherz, *Biophys. J.* **2004**, *87*, 1351–1359.
- [26] R. Pankov, *J. Cell Sci.* **2002**, *115*, 3861–3863.
- [27] E. Ruoslahti, *Cancer Metastasis Rev.* **1984**, *3*, 43–51.
- [28] M. Sessolo, D. Khodagholy, J. Rivnay, F. Maddalena, M. Gleyzes, E. Steidl, B. Buisson, G. G. Malliaras, *Adv. Mater.* **2013**, *25*, 2135–2139.
- [29] D. A. Bernards, G. G. Malliaras, G. E. S. Toombes, S. M. Gruner, *Appl. Phys. Lett.* **2006**, *89*, 053505.